

# DexGraspNet: A Large-Scale Robotic Dexterous Grasp Dataset for General Objects Based on Simulation

Ruicheng Wang<sup>1\*</sup>, Jialiang Zhang<sup>1\*</sup>, Jiayi Chen<sup>1,2</sup>, Yinzhen Xu<sup>1,2</sup>, Puhao Li<sup>2,3</sup>, Tengyu Liu<sup>2</sup>, He Wang<sup>1†</sup>

**Abstract**—Object grasping using dexterous hands is a crucial yet challenging task for robotic dexterous manipulation. Compared with the field of object grasping with parallel grippers, dexterous grasping is very under-explored, partially owing to the lack of a large-scale dataset. In this work, we present a large-scale simulated dataset, DexGraspNet, for robotic dexterous grasping, along with a highly efficient synthesis method for diverse dexterous grasping synthesis. Leveraging a highly accelerated differentiable force closure estimator, we, for the first time, are able to synthesize stable and diverse grasps efficiently and robustly. We choose ShadowHand, a dexterous gripper commonly seen in robotics, and generated 1.32 million grasps for 5355 objects, covering more than 133 object categories and containing more than 200 diverse grasps for each object instance, with all grasps having been validated by the physics simulator. Compared to the previous dataset generated by GraspIt!, our dataset has not only more objects and grasps, but also higher diversity and quality. Via performing cross-dataset experiments, we show that training several algorithms of dexterous grasp synthesis on our datasets significantly outperforms training on the previous one, demonstrating the large scale and diversity of DexGraspNet. We will release the data and tools upon acceptance.

## I. INTRODUCTION

Robotic object grasping is an important technology for many robotic systems. Recent years have witnessed great success in developing vision-based grasping methods [1–6] and large-scale datasets for parallel-jaw grippers, *e.g.*, synthetic object-centric dataset, ACRONYM [7], and real-world dataset of grasping in clutter, GraspNet [3].

Although simple and effective for pick-and-place, parallel-jaw grippers show certain limitations in dexterous object manipulation, *e.g.*, using scissors, due to their low DoFs. On the contrary, multi-fingered robotic hands, *e.g.*, ShadowHand [8], are human-like, designed with very high DoFs (26 for ShadowHand), and can attain more diverse grasp types. Those dexterous hands can support many complex and diverse manipulations, *e.g.*, solving Rubik’s cube [9], and can be used in task-specific grasping [10].

Arguably, dexterous grasping is the first step to dexterous manipulation. However, dexterous grasping is highly under-explored, compared to parallel grasping. One major obstacle is the lack of large-scale robotic dexterous grasping datasets required by learning-based methods. Up to now, the only dataset is provided by DDG [11], which contains only 6.9K grasps and 565 objects and is much smaller than

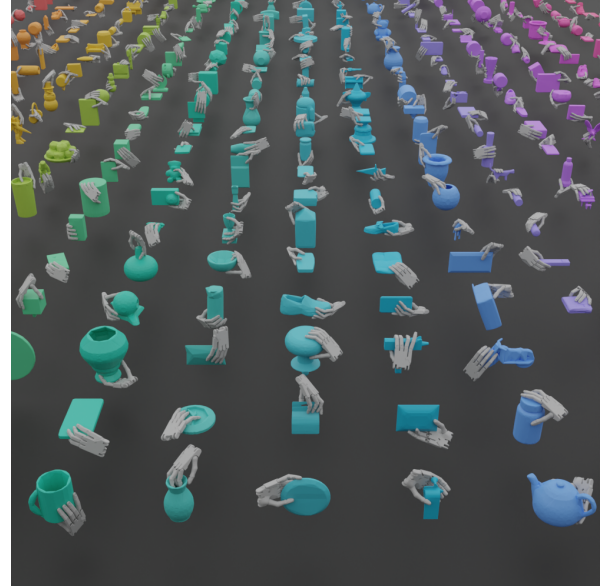


Fig. 1. **A visualization of DexGraspNet.** DexGraspNet contains 1.32M grasps of ShadowHand on 5355 objects, which is two orders and one order of magnitudes larger than the previous dataset from DDG. It features diverse types of grasping that can’t be achieved using GraspIt!.

the grasp datasets for parallel grippers, *e.g.*, GraspNet [3], ACRONYM [7]. Considering the high-DoF nature of the dexterous hand, the scale of dexterous grasping datasets needs to be significantly larger to generalize to unseen objects and cover the possible diverse grasping types. However, synthesizing diverse dexterous grasping is known to be both time-consuming and challenging to be correct and diverse.

In this work, we propose a large-scale robotic dexterous grasp dataset, DexGraspNet, that contains 1.32 million dexterous grasps for Shadow Hand on 5355 objects, with each object more than 200 diverse grasps. The objects are from diverse hand-scale object categories and collected from many synthetic and real datasets, including YCB [12], BigBIRD [13], Grasp [14], KIT [15], and Google’s scanned Object Dataset [16]. We normalize and clean these objects, remesh them into manifolds [17], and further compute collision meshes [18]. In addition, our dataset features diverse grasping types, compared to grasping generated by GraspIt! [19], and high quality, validated by Isaac Gym [20], which is a recently released physics simulator.

At the core of generating such a large dataset, we improve a dexterous hand grasping synthesis method based on differentiable force closure [26], making it much more efficient and robust. The original method proposes a differentiable

<sup>1</sup>Peking University

<sup>2</sup>Beijing Institute for General Artificial Intelligence

<sup>3</sup>Tsinghua University

\*Equal contribution

†Corresponding author: hewang@pku.edu.cn

TABLE I  
DATASETS FOR DEXTEROUS GRASPING

| Dataset            | Hand       | Observations | Sim./Real | Grasps       | Obj.(Cat.)       | Grasps per Obj. | Method           |
|--------------------|------------|--------------|-----------|--------------|------------------|-----------------|------------------|
| ObMan [21]         | MANO       | -            | Sim.      | 27k          | 2772(8)          | 10              | <i>GraspIt!</i>  |
| HO3D [22]          | MANO       | RGBD         | Real      | 77k          | 10               | >7k             | Estimation       |
| DexYCB [23]        | MANO       | RGBD         | Real      | 582K         | 20               | > <b>29k</b>    | Human Annotation |
| ContactDB [24]     | MANO       | RGBD+thermal | Real      | 3750         | 50               | 75              | Capture          |
| ContactPose [25]   | MANO       | RGBD         | Real      | 2306         | 25               | 92              | Capture          |
| DDGdata [11]       | ShadowHand | -            | Sim.      | 6.9k         | 565              | >100            | <i>GraspIt!</i>  |
| DexGraspNet (Ours) | ShadowHand | -            | Sim.      | <b>1.32M</b> | <b>5355(133)</b> | >200            | Optimization     |

energy term to approximate force closure, which is a sufficient condition to achieve physically plausible grasping, and optimizes it to obtain grasping poses. Note that it is highly non-trivial for us to synthesize a large-scale dataset simply using [26], due to its several limitations on low success rate and slow convergence. Therefore, we propose several critical improvements to [26] for speeding up the synthesis and improving its quality, including a better pose initialization, an alternative to compute penetration energy and signed distances, and energy terms to prevent self-penetration and out-of-limit joint angles. For synthesizing 10000 valid grasps, we speed up from 400 GPU hours to 7 GPU hours.

To verify the advantage of our dataset over the one from DDG, we train two dexterous grasping algorithms on our dataset and DDG. The cross-dataset experiments confirm that training on our dataset yields better grasping quality and higher diversity. Also, the great diversity of the hand grasps from our dataset leaves huge improvement space for future dexterous grasping algorithms.

## II. RELATED WORK

Researches in grasping can be broadly categorized by the types of end effectors involved. The most thoroughly studied ones are the suction cup and parallel jaw grippers, whose grasp pose can be defined by a 7D vector at most, including 3D for translation, 3D for rotation, and 1D for the width between the two fingers. Dexterous robotic hands with three or more fingers such as ShadowHand [8] and humanoid hands such as MANO [27] require more complex descriptors, sometimes up to 24DoF as in ShadowHand [8]. In this paper, we are dedicated to researches on the latter type. To bridge the gap between humanoid hands and robotic hands, numerous researches have shown the efficacy of retargeting humanoid hand poses to dexterous robotic hands [28–31].

### A. Analytical Grasping

Early researches in dexterous grasping focus on optimizing grasping poses to form force closure that can resist external forces and torques [32–35].

Due to the complexity of computing hand kinematics and testing force closure, many works were devoted to simplifying the search space [36–38]. As a result, these methods were applicable to restricted settings and can only produce limited types of grasping poses. Another stream of work [39–41] looks for simplifying the optimization process with an auxiliary function. [26] proposed to use a differentiable estimator of the force closure metric to synthesize diverse grasping poses for arbitrary hands.

### B. Data-Driven Grasping

Recent works shift their focus to data-driven methods. Given an object, the most straightforward approach is to directly generate the pose vectors of the grasping hand [42–46]. A refinement step is usually implemented in these methods to remove inconsistencies such as penetration.

Other methods take an indirect approach that involves generating an intermediate representation first. Existing methods use contact points [47–49], contact maps [28, 29, 50–52], and occupancy fields [53] as the intermediate representations. The methods then obtain the grasping poses via optimization [47, 48, 51, 53], planning [50], RL policies [29, 49], or another generative model [52].

Compared to most analytical methods, data-driven methods show improved inference speed and diversity of generated grasping poses. However, the diversity is still limited by the training data.

### C. Dexterous Grasp Datasets

Dexterous grasping is impossibly difficult to annotate for its overwhelming degrees of freedom. Most existing works are trained on programmatically synthesized grasping poses [11, 21, 45, 54] using the *GraspIt!* [19] planner. The planner first searches the eigengrasp space for pregrasp poses that cross a threshold. Then, the planner squeezes all fingers in the selected pregrasp poses to construct a firm grasp. Since the initial search is performed in the low dimensional eigengrasp space, the resulting data follows a narrow distribution and cannot cover the full dexterity of multi-finger hands.

More recent works leverage the increasing capacity of computer vision to collect human hand poses when interacting with the object. HO3D [22, 55] computes the ground truth 3D hand pose for images from 2D hand keypoint annotations. The method resolves ambiguities by considering physics constraints in hand-object interactions and hand-hand interactions. DexYCB [23] and ContactPose [25] solves the 3D hand shape from multi-view RGBD camera recordings. Latest datasets [56–58] use optical motion capture systems to track hand and object shapes during interactions. While these methods produce natural and smooth interaction demonstrations, the data is restricted to humanoid hand structures and daily hand poses.

In addition, ContactDB [24] and ContactPose [25] leverage IR cameras to collect contact maps on object surfaces.

### III. DATASET GENERATION

#### A. Object Preparation

We use Computer-Aided-Design (CAD) models and scanned models for object meshes: YCB [12], BigBIRD [13], Grasp [14], KIT [15], and Google's scanned Object Dataset [16] are scanned model repositories without category labels, from which we select 1375 objects into our category-novel set; ShapeNetCore and ShapeNetSem [59, 60] contain CAD models with category labels, from which we select 3980 objects in 133 categories into our category-level set.

To avoid extremely large or small object sizes, we first normalize the meshes by their scales and then augment each object by uniformly scaling them using 5 fixed sizes. For simulation purposes, we create a collision mesh for every object mesh through convex decomposition using CoACD [18]. These collision meshes are used both in grasp generation and grasp validation.

#### B. Grasp Generation

1) *Assumptions and Notations:* During grasp generation, we keep the objects in their canonical space with zero-centered translation. To parameterize dexterous grasps, we use tuples  $g = (T, R, \theta)$ , where  $T \in \mathbb{R}^3$  and  $R \in SO(3)$  gives the global hand pose, and  $\theta \in \mathbb{R}^{22}$  describes the  $d$  joint angles ( $d = 22$  for Shadow Hand). Given the URDF of the dexterous hand, we can use  $g$  to compute the hand mesh  $H$  via forward kinematics. In the generation process, we need to consider the contact points. Following [26]'s idea that fewer contact candidates lead to faster convergence, we first manually select 140 contact candidates from the surface of the hand and empirically pick  $n = 4$  as the number of contact points, denoted by  $x \in \mathbb{R}^{n \times 3}$ . We then augment our grasp tuple to  $g' = (T, R, \theta, x)$ , with  $x$  representing the  $n = 4$  contact points. Given object mesh  $O$ , the contact normal vectors  $c \in \mathbb{R}^{n \times 3}$  can be computed from  $x$ . Note that  $x$  is an intermediate variable used by the grasp generation algorithm and is discarded after the algorithm finishes.

2) *Review of Differentiable Force Closure:* Our dexterous grasp generation method is mainly built on the original work [26], in which they proposed a novel differentiable force closure estimator as an energy term and used optimization to synthesize grasps. The proposed differentiable force closure term, which encourages a set of contact points to form force closure, can be expressed as

$$E_{fc} = \|Gc\|_2 \quad (1)$$

where

$$G = \begin{bmatrix} I_3 & \cdots & I_3 \\ [x_1]_{\times} & \cdots & [x_n]_{\times} \end{bmatrix}$$

$$[x_i]_{\times} = \begin{bmatrix} 0 & -x_i^{(z)} & x_i^{(y)} \\ x_i^{(z)} & 0 & -x_i^{(x)} \\ -x_i^{(y)} & x_i^{(x)} & 0 \end{bmatrix}$$

A pair of attraction and repulsion energy functions were introduced to ensure contact and prevent penetration:

$$E_{dis} = \sum_{i=1}^n d(x_n, O), E_{pen} = \sum_{v \in S(H)} [v \in O] d(v, O) \quad (2)$$

where  $S(H)$  was the surface point cloud of the hand mesh  $H$ ,  $d(\cdot, \cdot)$  was the point-to-mesh distance and  $[v \in O] = 1$  if point  $v$  was inside object mesh  $O$ . They also used an energy function  $E_{prior}$  to keep the hand in a natural state. The complete energy function was as follows:

$$E = E_{fc} + w_{dis}E_{dis} + w_{pen}E_{pen} + w_{prior}E_{prior} \quad (3)$$

They designed a modified MALA optimization algorithm to minimize the energy  $E$  over the augmented grasp tuple  $g' = (T, R, \theta, x)$ . The algorithm took an initial hand pose  $g'_0$ , which was randomly initialized. Then, in each iteration,  $T, R, \theta$  were updated according to Langevin dynamics, and  $x$  was randomly re-sampled with a small probability. The update was accepted or rejected stochastically by the Metropolis-Hastings rule. The optimization ends after 10000 steps. For more details, please refer to [26].

3) *Our Method:* Though [26] took a great step forward, it is still quite hard to obtain a large-scale grasp dataset directly using their method due to three reasons: 1. the algorithm suffers from a low success rate and slow convergence; 2. most object meshes we use have no thickness due to the poor quality of the object dataset, making it impossible to compute penetration energy; 3. due to random initialization, some generated grasping poses may look twisted.

To overcome these issues, we propose several ways to improve efficiency, effectiveness, and robustness of the original algorithm:

First, we propose an initialization strategy that can greatly improve the success rate and speed up the convergence. We find that their optimization algorithm's success rate drops dramatically when the initial hand is closed. This motivates us to introduce two constraints to the initialization strategy: 1. the five fingers should be opened to form a space for grasping; 2. the hand should face the object.

More specifically, we manually choose a canonical hand pose  $\theta_m$ , as shown in Figure 2, then jitter each joint angle within its limit using the truncated normal distribution. Then, on each object mesh, we first take its convex hull, then push every vertex of the hull away from the origin by  $0.2m$  to obtain the inflated convex hull. Next, we sample a random point  $p$  on the surface of the inflated convex hull, and compute the direction vector from  $p$  to its nearest point on the original object mesh, then jitter this direction vector within a cone and get  $\vec{n}$ . Finally, the hand is moved to  $p$ , and rotated to face the same direction as  $\vec{n}$ , then push away from the object mesh along  $\vec{n}$  by a random distance, and rotated around  $\vec{n}$  randomly.

The resulting initial hand pose  $(T_0, R_0, \theta_0)$  can be easily optimized to a grasp pose, thus raising the success rate of the algorithm. Moreover, we can guarantee that for each object, if we sample enough initial hands, they can surround the

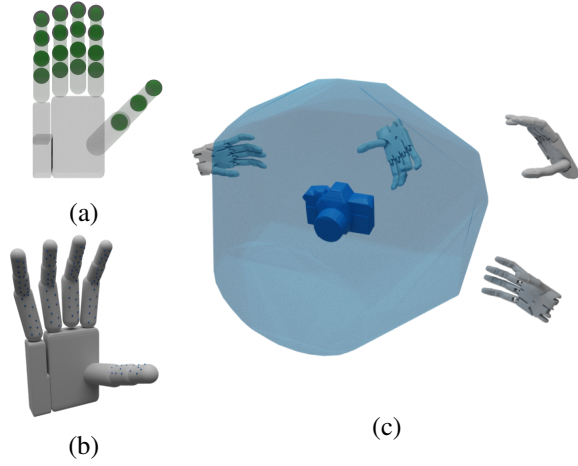


Fig. 2. (a) Green points are manually selected to compute the self-penetration energy, with the radius of  $\delta = 1\text{cm}$ . (b) Dexterous hand in the canonical pose for initialization. (c) Sketch of the initialization process: 1. sample points on the surface of the enlarged convex hull of the object, shown in blue; 2. put hands on the sampled points and jitter the global 6D hand pose and joint angles.

object densely and evenly, so we can generate diverse data. Also, we found that using our strategy, the final grasp poses look more natural.

Second, we propose an alternative way to compute penetration energy that can make the algorithm more robust to thin object meshes of low quality. In practice, the original algorithm will fail completely when the object mesh has no thickness because the penetration energy will always be zero. Therefore, instead of taking the point cloud from the hand, we take it from the object and compute each point’s distance to the hand mesh. We call this the reverse penetration energy. It doesn’t require the object mesh to have any thickness at all, allowing us to process more objects.

Third, we use a better implementation of  $E_{\text{prior}}$ , inspired by [52] to penalize self penetration and out-of-limit joint angles:

$$E_{\text{spen}} = \sum_{p \in P(H)} \sum_{q \in P(H)} [p \neq q] \max(\delta - d(p, q), 0) \quad (4)$$

$$E_{\text{joints}} = \sum_{i=1}^d (\max(\theta_i - \theta_i^{\max}, 0) + \max(\theta_i^{\min} - \theta_i, 0)) \quad (5)$$

This adds to our final energy function:

$$E_{\text{fc}} + w_{\text{dis}} E_{\text{dis}} + w_{\text{pen}} E_{\text{pen}} + w_{\text{spen}} E_{\text{spen}} + w_{\text{joints}} E_{\text{joints}} \quad (6)$$

where  $w_{\text{dis}} = 100$ ,  $w_{\text{pen}} = 100$ ,  $w_{\text{spen}} = 10$ ,  $w_{\text{joints}} = 1$ .

Another minor difference between our implementation and [26] lies in the optimization algorithms. Because our initialization strategy has already raised the success rate of the algorithm to an acceptable level, we simplify MALA and use simple gradient descent to update  $T, R, \theta$  during each optimization step. In our settings, the optimization process converges in less than 6000 iterations, which reduces almost half of the original iterations.

Finally, we use a modified version of Kaolin [61] instead of DeepSDF [62] to compute point-to-mesh signed distances,

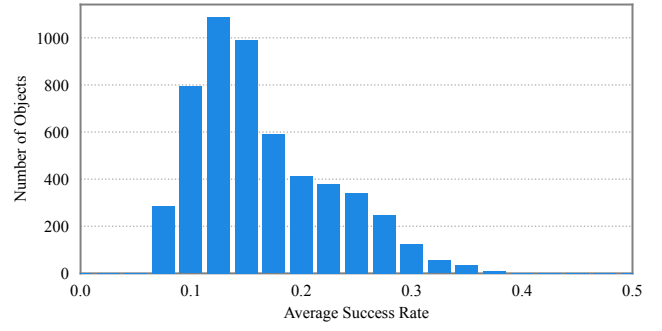


Fig. 3. Distribution of the object numbers with respect to the average success rate for each object after the optimization converges. Note that we only save those success grasps as our dataset.

which eliminates the need for pretraining category level DeepSDF networks, and significantly reduces the memory cost when optimizing grasps.

### C. Grasp Validation

To filter out those bad results after the optimization converges, we validate all of the grasps in a physical simulator Isaac Gym [20] with PhysX as the basic physics engine. We first initialize the gripper using the final grasp parameters. Then, in order to apply active forces on the object, we slightly move the contacting links of the gripper along the normal of its contact point, and set the moved pose as target positions for positional control. Finally, gravity with a magnitude of  $9.8m/s^2$  is added to the scene. A grasp is considered successful if the gripper is still in contact with the object after 100 simulation steps under all 6 axis-aligned directions of gravity. The distribution of the object number with respect to the average success rate for each object is shown in Fig. 3. Moreover, if the max penetration depth exceeds 0.1cm, we also consider the grasp as a failure. Finally, we only save those grasps who pass both the simulation validation and the penetration validation as our dataset.

### D. Comparison of Computational Cost

Finally, we compare our improved version versus the original algorithm [26] in computational cost for the dataset generation. On A100 graphics cards, Our algorithm takes 74min to optimize 10000 grasps for 6000 steps, out of which about 18% are considered valid under our settings. The original algorithm of [26] takes 37min on NVIDIA 3090 to optimize 512 grasps for 10000 steps, out of which about 3% are considered valid. It took us 950 GPU hours to generate 1.32 million valid grasps, which would have taken the original algorithm 50000 GPU hours to compute. This speed-up is contributed by faster convergence, smaller memory (which leads to bigger batch size), and a higher success rate.

## IV. DATASET ANALYSIS AND COMPARISON

With the improved pipeline described above, we finally generate more than 200 grasps per object, which sums up to 1.32 million grasps in total. To the best of our knowledge,



Fig. 4. Visualization of the diverse grasps on the diverse objects from DexGraspNet.

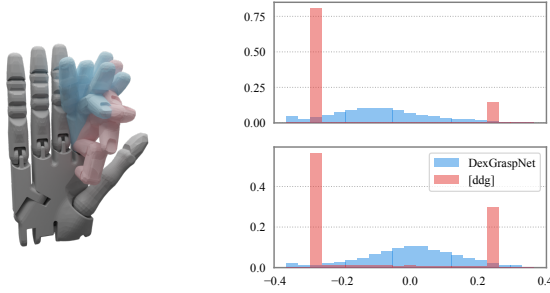


Fig. 5. Diversity comparison between DexGraspNet and DDGdata. Left: we sample different grasp poses and draw theirs in red and blue. For visual simplicity, we only show the index finger, but all five fingers share the same phenomenon. The fingers of DDGdata all distribute on a fan, while our data has higher freedom. Right: Probability distribution of two joint angles over all grasp poses. DDGdata suffers from mode collapse.

this is by far the largest grasping dataset for ShadowHand. It has the largest number of objects, categories, grasps per object, and total grasps. Apart from scale, we also argue that our dataset possesses good grasping quality and high pose diversity. We will verify our arguments by comparing DexGraspNet with the dataset proposed in DDG [11] (in short DDGdata), a grasping dataset for ShadowHand generated by *GraspIt!* [19], on two aspects below.

First, we concluded that DexGraspNet has more diverse grasping poses. As shown in Figure 5, since the planner in *GraspIt!* simply closes joints to generate grasping poses and the closing direction is always the same, their grasping poses only have one freedom for the root joint angle of each finger, resulting in the lack of diversity. What’s more, the angles of many joints in DDGdata often collapse to either the upper or lower limit of those joints, which is also caused by their simple generation strategy and contributes to a serious loss of diversity. In contrast, our optimization-based method doesn’t have this problem and can generate diverse grasping poses with higher dexterity, as shown in Figure 4. We further use the mean entropy of each joint angle to model the diversity quantitatively, as shown in Table II.

Second, we show our DexGraspNet has higher grasp quality than DDGdata by computing the  $Q_1$  or epsilon value [63]. Intuitively,  $Q_1$  is the norm of the smallest wrench that can destabilize the grasp:

$$Q_1 = \text{inscribed sphere radius of } \text{ConvexHull}(\cup_i w_i) \quad (7)$$

where  $\{w_i\}_i$  are the contact friction cone wrenches. We choose 1mm as the contact threshold, and allow at most

TABLE II  
STATISTICS OF  $Q_1$  AND ENTROPY

| Dataset     | 100% $Q_1$ mean | best 10% $Q_1$ mean | $H$ mean     |
|-------------|-----------------|---------------------|--------------|
| DDGdata     | 0.0712          | 0.2277              | 4.246        |
| DexGraspNet | <b>0.1145</b>   | <b>0.2533</b>       | <b>5.962</b> |

one contact point for each link to save computational time. The results are shown in Table II. We can find that the average value of our dataset is significantly better than that of DDGdata. It is worth noting that the whole generation pipeline does not directly optimize this metric.

## V. BENCHMARKS

We benchmark two methods of dexterous grasp synthesis, DDG [11] and GraspTTA [42], on our dataset, and compare them with the same methods trained on DDGdata [11].

### A. Benchmark Methods

Deep Differentiable Grasp (DDG) [11] designs a differentiable  $Q_1$  metric, which generalizes the standard  $Q_1$  metric to the case when the gripper is not in contact with objects. With this generalized  $Q_1$  metric, they are able to supervise the neural network to predict fine grasp end-to-end. Their network takes 5 depth images of the object as input and directly regresses the 6D pose and joint angles of the ShadowHand. To ease learning, they divide the training process into two stages. In the first stage, they only use the loss of the grasp poses, and in the second stage, they fine-tune the network with differentiable  $Q_1$  loss and other losses to avoid penetration and pull the hand closer to the object. We follow their data pre-process pipeline to generate the BVH representation and depth images of our objects, and train the network with official settings on each dataset.

Another work GraspTTA (short for Test-Time Adaptation) [42] proposes to synthesize high-quality grasps by ensuring the contact consistency between the hand and the object. They design two networks, one is a CVAE [64] to synthesize grasps, and the other is a contact net to predict the contact regions of the object. During training, those two networks are trained separately. During testing, a grasp is synthesized in a two-stage process. First, the CVAE takes the object point cloud as condition, samples a latent code, and then decodes the hand 6D global pose and joint angles, which can be further transformed into the hand point cloud through forward kinematics. Second, the contact net takes both the object and the hand point cloud to predict a target



TABLE III  
BENCHMARKS OF THE GRASP QUALITY

| Method (Training Dataset) | Tested on DexGraspNet |                  |                  | Tested on DDGdata  |                  |                  |
|---------------------------|-----------------------|------------------|------------------|--------------------|------------------|------------------|
|                           | success $\uparrow$    | $Q_1$ $\uparrow$ | pen $\downarrow$ | success $\uparrow$ | $Q_1$ $\uparrow$ | pen $\downarrow$ |
| DDG (DDGdata)             | 57.4                  | 0.0493           | 0.353            | 56.4               | 0.0461           | 0.333            |
| DDG (DexGraspNet)         | <b>67.5</b>           | <b>0.0582</b>    | <b>0.173</b>     | <b>75.9</b>        | <b>0.0524</b>    | <b>0.134</b>     |
| GraspTTA (DDGdata)        | 17.1                  | 0.0126           | 0.720            | 23.7               | 0.0265           | 0.666            |
| GraspTTA (DexGraspNet)    | <b>24.5</b>           | <b>0.0271</b>    | <b>0.678</b>     | <b>39.3</b>        | <b>0.0790</b>    | <b>0.547</b>     |

contact map, and optimizes the hand parameters to minimize the difference between the current contact map and the target contact map. We re-implement GraspTTA on ShadowHand, process the data from DexGraspNet and DDGdata in the same way as in [42], and train the networks on each dataset for the same number of iterations.

### B. Experiments and Results

We report following metrics for evaluation. 1) **Simulation success rate(%) in Isaac Gym**. We use an easier variation of Sec. III-C, in which a grasp is considered valid if it can withstand at least one of the six gravity directions and has a maximal penetration less than 5mm, because the original metric was too strict for baselines. 2) **Mean  $Q_1$**  [63], which is introduced in Sec. IV. Since these methods cannot guarantee exact contact, we relax the contact threshold to 1cm. Particularly, if penetration depth of a grasp is greater than 5mm, the  $Q_1$  metric is not well defined, so we manually set  $Q_1$  of these results to 0. 3) **Maximal penetration depth(cm)**. This is defined as the maximal penetration depth from the object point cloud to hand meshes.

The main results are presented in Table III. We compare models trained on DexGraspNet with models trained on DDGdata, finding that no matter which baseline, test set, or metric we use, the former always scores higher. From this result, we conclude that learning-based grasping methods achieve higher performance when they are trained under our dataset. Table III also shows that the output of DDG has higher quality than GraspTTA most of the time. More specifically, GraspTTA suffers severely from penetration.

Apart from grasp quality, we use joint angle entropy as a metric to evaluate the diversity of the grasps generated by the two methods. Fixing the method and test set, Table IV shows that models trained on DexGraspNet always have higher mean entropy and lower standard deviation of entropy than models trained on DDGdata, which means that DexGraspNet improves the diversity of grasping methods. Fixing the train set and test set, we find that GraspTTA has higher diversity than DDG. This phenomenon is natural since GraspTTA has test time optimization and DDG is a feed-forward model. Even though DexGraspNet promotes DDG’s ability to generate diverse hand poses, DDG’s entropy is still lower than DexGraspNet’s entropy, meaning DDG cannot fully recover DexGraspNet’s diversity. Interestingly, GraspTTA yields an entropy higher than DexGraspNet when trained and tested on DexGraspNet. But on the other hand, GraspTTA’s success rate is too low, so having a high entropy doesn’t necessarily mean that GraspTTA actually learned diverse grasping. In

conclusion, existing grasping methods cannot fully learn the highly diverse grasp poses of DexGraspNet, while keeping a reasonable success rate at the same time.

Taking both stability and diversity into consideration, we emphasize the following observations. Stability and diversity are contradictory to a degree, and both are important metrics for grasping. DDG and GraspTTA each have their own preference and trade-off. However, non of the existing methods can perform well on both metrics. Moreover, since stability has already been solved nicely by parallel grippers, we argue that dexterous grippers should delve deeper into diversity and dexterity. We release DexGraspNet at this time point, in the hope that its scale, quality, and diversity can help future methods tackle the task of dexterous grasping, and exploit the true potential of the dexterous gripper.

TABLE IV  
BENCHMARKS OF THE GRASP DIVERSITY

| Method (Training Dataset) | DexGraspNet  |              | DDGdata      |              |
|---------------------------|--------------|--------------|--------------|--------------|
|                           | $H$ mean     | $H$ std      | $H$ mean     | $H$ std      |
| DDG (DDGdata)             | 4.958        | 2.653        | 3.709        | 1.942        |
| DDG (DexGraspNet)         | <b>5.683</b> | <b>1.993</b> | <b>4.272</b> | <b>1.287</b> |
| GraspTTA (DDGdata)        | 5.952        | 0.934        | 5.837        | 1.047        |
| GraspTTA (DexGraspNet)    | <b>6.111</b> | <b>0.569</b> | <b>5.947</b> | <b>0.528</b> |

## VI. LIMITATIONS

By comparing the grasps in our dataset with the taxonomy from [65], we notice that our dataset cannot cover every grasping type described. Since the optimization step tends to pull every candidate point closer to the object, the final grasps are always contact-rich, or power grasps. Therefore, precision grasps hardly appear, which represents the dexterity of multi-finger robotic hands. Additionally, our method lacks semantic guidance, which makes it hard to generate functional grasps, *e.g.* picking up the mug through its handle. Precision grasps and functional grasps remain important issues for us to explore.

## VII. CONCLUSIONS

In this paper, we present a large-scale dexterous grasping dataset, DexGraspNet based on simulation. This dataset features more physical stability and higher diversity than previous datasets. Trained on DexGraspNet, previous grasp synthesis methods can achieve consistent improvements in both stability and diversity. However, compared to the current progress in non-dexterous grasping synthesis, we argue that dexterous grasping synthesis still has a large room for research, and we hope DexGraspNet could aid future researchers in this field.

## REFERENCES

- [1] M. Breyer, J. J. Chung, L. Ott, R. Siegwart, and J. Nieto, “Volumetric grasping network: Real-time 6 dof grasp detection in clutter,” *arXiv preprint arXiv:2101.01132*, 2021.
- [2] M. Sundermeyer, A. Mousavian, R. Triebel, and D. Fox, “Contact-graspnet: Efficient 6-dof grasp generation in cluttered scenes,” in *2021 IEEE International Conference on Robotics and Automation (ICRA)*. IEEE, 2021, pp. 13 438–13 444.
- [3] H.-S. Fang, C. Wang, M. Gou, and C. Lu, “Graspnet-1billion: A large-scale benchmark for general object grasping,” in *Proceedings of the IEEE/CVF conference on computer vision and pattern recognition*, 2020, pp. 11 444–11 453.
- [4] M. Gou, H.-S. Fang, Z. Zhu, S. Xu, C. Wang, and C. Lu, “Rgb matters: Learning 7-dof grasp poses on monocular rgbd images,” in *Proceedings of the International Conference on Robotics and Automation (ICRA)*, 2021.
- [5] C. Wang, H.-S. Fang, M. Gou, H. Fang, J. Gao, and C. Lu, “Graspness discovery in clutters for fast and accurate grasp detection,” in *Proceedings of the IEEE/CVF International Conference on Computer Vision (ICCV)*, October 2021, pp. 15 964–15 973.
- [6] H. Fang, H.-S. Fang, S. Xu, and C. Lu, “Transcg: A large-scale real-world dataset for transparent object depth completion and a grasping baseline,” *IEEE Robotics and Automation Letters*, pp. 1–8, 2022.
- [7] C. Eppner, A. Mousavian, and D. Fox, “ACRONYM: A large-scale grasp dataset based on simulation,” in *2021 IEEE Int. Conf. on Robotics and Automation, ICRA*, 2020.
- [8] “ShadowRobot,” URL <https://www.shadowrobot.com/dexterous-hand-series/>, 2005.
- [9] I. Akkaya, M. Andrychowicz, M. Chociej, M. Litwin, B. McGrew, A. Petron, A. Paino, M. Plappert, G. Powell, R. Ribas, *et al.*, “Solving rubik’s cube with a robot hand,” *arXiv preprint arXiv:1910.07113*, 2019.
- [10] M. Kokic, J. A. Stork, J. A. Haustein, and D. Kragic, “Affordance detection for task-specific grasping using deep learning,” in *2017 IEEE-RAS 17th International Conference on Humanoid Robotics (Humanoids)*. IEEE, 2017, pp. 91–98.
- [11] M. Liu, Z. Pan, K. Xu, K. Ganguly, and D. Manocha, “Deep differentiable grasp planner for high-dof grippers,” *arXiv preprint arXiv:2002.01530*, 2020.
- [12] B. Calli, A. Singh, J. Bruce, A. Walsman, K. Konolige, S. Srinivasa, P. Abbeel, and A. M. Dollar, “Yale-cmu-berkeley dataset for robotic manipulation research,” *The International Journal of Robotics Research*, vol. 36, no. 3, pp. 261–268, 2017.
- [13] A. Singh, J. Sha, K. S. Narayan, T. Achim, and P. Abbeel, “Bigbird: A large-scale 3d database of object instances,” in *2014 IEEE international conference on robotics and automation (ICRA)*. IEEE, 2014, pp. 509–516.
- [14] D. Kappler, J. Bohg, and S. Schaal, “Leveraging big data for grasp planning,” in *2015 IEEE international conference on robotics and automation (ICRA)*. IEEE, 2015, pp. 4304–4311.
- [15] A. Kasper, Z. Xue, and R. Dillmann, “The kit object models database: An object model database for object recognition, localization and manipulation in service robotics,” *The International Journal of Robotics Research*, vol. 31, no. 8, pp. 927–934, 2012.
- [16] L. Downs, A. Francis, N. Koenig, B. Kinman, R. Hickman, K. Reymann, T. B. McHugh, and V. Vanhoucke, “Google scanned objects: A high-quality dataset of 3d scanned household items,” *arXiv preprint arXiv:2204.11918*, 2022.
- [17] J. Huang, Y. Zhou, and L. Guibas, “Manifoldplus: A robust and scalable watertight manifold surface generation method for triangle soups,” *arXiv preprint arXiv:2005.11621*, 2020.
- [18] X. Wei, M. Liu, Z. Ling, and H. Su, “Approximate convex decomposition for 3d meshes with collision-aware concavity and tree search,” *arXiv preprint arXiv:2205.02961*, 2022.
- [19] A. T. Miller and P. K. Allen, “Graspit! a versatile simulator for robotic grasping,” *IEEE Robotics & Automation Magazine*, 2004.
- [20] J. Liang, V. Makovychuk, A. Handa, N. Chentanez, M. Macklin, and D. Fox, “Gpu-accelerated robotic simulation for distributed reinforcement learning,” in *Conference on Robot Learning*. PMLR, 2018, pp. 270–282.
- [21] Y. Hasson, G. Varol, D. Tzionas, I. Kalevtykh, M. J. Black, I. Laptev, and C. Schmid, “Learning joint reconstruction of hands and manipulated objects,” in *Conference on Computer Vision and Pattern Recognition (CVPR)*, 2019.
- [22] S. Hampali, M. Rad, M. Oberweger, and V. Lepetit, “Honnotate: A method for 3d annotation of hand and object poses,” in *Conference on Computer Vision and Pattern Recognition (CVPR)*, 2020.
- [23] Y.-W. Chao, W. Yang, Y. Xiang, P. Molchanov, A. Handa, J. Tremblay, Y. S. Narang, K. Van Wyk, U. Iqbal, S. Birchfield, *et al.*, “Dexycb: A benchmark for capturing hand grasping of objects,” in *Proceedings of the IEEE/CVF Conference on Computer Vision and Pattern Recognition*, 2021, pp. 9044–9053.
- [24] S. Brahmabhatt, C. Ham, C. C. Kemp, and J. Hays, “Contactdb: Analyzing and predicting grasp contact via thermal imaging,” in *Conference on Computer Vision and Pattern Recognition (CVPR)*, 2019.
- [25] S. Brahmabhatt, C. Tang, C. D. Twigg, C. C. Kemp, and J. Hays, “Contactpose: A dataset of grasps with object contact and hand pose,” in *European Conference on Computer Vision (ECCV)*, 2020.
- [26] T. Liu, Z. Liu, Z. Jiao, Y. Zhu, and S.-C. Zhu, “Synthesizing diverse and physically stable grasps with arbitrary hand structures using differentiable force closure estimator,” *IEEE Robotics and Automation Letters (RA-L)*, 2021.
- [27] J. Romero, D. Tzionas, and M. J. Black, “Embodied hands: Modeling and capturing hands and bodies together,” *ACM Transactions on Graphics (TOG)*, 2017.
- [28] S. Brahmabhatt, A. Handa, J. Hays, and D. Fox, “Contactgrasp: Functional multi-finger grasp synthesis from contact,” in *International Conference on Intelligent Robots and Systems (IROS)*, 2019.
- [29] P. Mandikal and K. Grauman, “Learning dexterous grasping with object-centric visual affordances,” in *2021 IEEE International Conference on Robotics and Automation (ICRA)*. IEEE, 2021, pp. 6169–6176.
- [30] Y. Qin, H. Su, and X. Wang, “From one hand to multiple hands: Imitation learning for dexterous manipulation from single-camera teleoperation,” *arXiv preprint arXiv:2204.12490*, 2022.
- [31] J. Ye, J. Wang, B. Huang, Y. Qin, and X. Wang, “Learning continuous grasping function with a dexterous hand from human demonstrations,” *arXiv preprint arXiv:2207.05053*, 2022.
- [32] A. Rodriguez, M. T. Mason, and S. Ferry, “From caging to grasping,” *International Journal of Robotics Research (IJRR)*, vol. 31, no. 7, pp. 886–900, 2012.
- [33] D. Prattichizzo, M. Malvezzi, M. Gabiccini, and A. Bicchi, “On the manipulability ellipsoids of underactuated robotic hands with compliance,” *Robotics and Autonomous Systems*, vol. 60, no. 3, pp. 337–346, 2012.
- [34] C. Rosales, R. Suárez, M. Gabiccini, and A. Bicchi, “On the synthesis of feasible and prehensile robotic grasps,” in *International Conference on Robotics and Automation (ICRA)*, 2012.
- [35] R. M. Murray, *A mathematical introduction to robotic manipulation*. CRC press, 2017.
- [36] J. Ponce, S. Sullivan, J.-D. Boissonnat, and J.-P. Merlet, “On characterizing and computing three- and four-finger force-closure grasps of polyhedral objects,” in *International Conference on Robotics and Automation (ICRA)*, 1993.
- [37] J. Ponce, S. Sullivan, A. Sudsang, J.-D. Boissonnat, and J.-P. Merlet, “On computing four-finger equilibrium and force-closure grasps of polyhedral objects,” *International Journal of Robotics Research (IJRR)*, vol. 16, no. 1, pp. 11–35, 1997.
- [38] J.-W. Li, H. Liu, and H.-G. Cai, “On computing three-finger force-closure grasps of 2-d and 3-d objects,” *IEEE Transactions on Robotics and Automation*, vol. 19, no. 1, pp. 155–161, 2003.
- [39] Y. Zheng and C.-M. Chew, “Distance between a point and a convex cone in  $n$ -dimensional space: Computation and applications,” *Transactions on Robotics (T-RO)*, vol. 25, no. 6, pp. 1397–1412, 2009.
- [40] H. Dai, A. Majumdar, and R. Tedrake, “Synthesis and optimization of force closure grasps via sequential semidefinite programming,” in *Robotics Research*. Springer, 2018, pp. 285–305.
- [41] Y.-H. Liu, “Qualitative test and force optimization of 3-d frictional form-closure grasps using linear programming,” *IEEE Transactions on Robotics and Automation*, vol. 15, no. 1, pp. 163–173, 1999.
- [42] H. Jiang, S. Liu, J. Wang, and X. Wang, “Hand-object contact consistency reasoning for human grasps generation,” in *International Conference on Computer Vision (ICCV)*, 2021.
- [43] E. Corona, A. Pumarola, G. Alenya, F. Moreno-Noguer, and G. Rogez, “Ganhand: Predicting human grasp affordances in multi-object scenes,” in *Conference on Computer Vision and Pattern Recognition (CVPR)*, 2020.

- [44] J. Lundell, E. Corona, T. N. Le, F. Verdoja, P. Weinzaepfel, G. Rogez, F. Moreno-Noguer, and V. Kyrki, "Multi-fingan: Generative coarse-to-fine sampling of multi-finger grasps," in *International Conference on Robotics and Automation (ICRA)*, 2021.
- [45] J. Lundell, F. Verdoja, and V. Kyrki, "Ddgc: Generative deep dexterous grasping in clutter," *IEEE Robotics and Automation Letters (RA-L)*, 2021.
- [46] L. Yang, X. Zhan, K. Li, W. Xu, J. Li, and C. Lu, "Cpf: Learning a contact potential field to model the hand-object interaction," in *Proceedings of the IEEE/CVF International Conference on Computer Vision*, 2021, pp. 11 097–11 106.
- [47] L. Shao, F. Ferreira, M. Jorda, V. Nambiar, J. Luo, E. Solowjow, J. A. Ojea, O. Khatib, and J. Bohg, "Unigrasp: Learning a unified model to grasp with multifingered robotic hands," *IEEE Robotics and Automation Letters (RA-L)*, 2020.
- [48] A. Wu, M. Guo, and C. K. Liu, "Learning diverse and physically feasible dexterous grasps with generative model and bilevel optimization," *arXiv preprint arXiv:2207.00195*, 2022.
- [49] K. Li, N. Baron, X. Zhang, and N. Rojas, "Efficientgrasp: A unified data-efficient learning to grasp method for multi-fingered robot hands," *IEEE Robotics and Automation Letters*, vol. 7, no. 4, pp. 8619–8626, 2022.
- [50] J. Varley, J. Weisz, J. Weiss, and P. Allen, "Generating multi-fingered robotic grasps via deep learning," in *2015 IEEE/RSJ international conference on intelligent robots and systems (IROS)*. IEEE, 2015, pp. 4415–4420.
- [51] D. Turpin, L. Wang, E. Heiden, Y.-C. Chen, M. Macklin, S. Tsogkas, S. Dickinson, and A. Garg, "Grasp'd: Differentiable contact-rich grasp synthesis for multi-fingered hands," 2022.
- [52] T. Zhu, R. Wu, X. Lin, and Y. Sun, "Toward human-like grasp: Dexterous grasping via semantic representation of object-hand," in *Proceedings of the IEEE/CVF International Conference on Computer Vision*, 2021, pp. 15 741–15 751.
- [53] K. Karunratanakul, J. Yang, Y. Zhang, M. Black, S. Tang, and K. Muandet, "Grasping field: Learning implicit representations for human grasps," in *International Conference on 3D Vision (3DV)*, 2020.
- [54] C. Goldfeder, M. Ciocarlie, H. Dang, and P. K. Allen, "The columbia grasp database," in *2009 IEEE international conference on robotics and automation*. IEEE, 2009, pp. 1710–1716.
- [55] S. Hampali, S. D. Sarkar, M. Rad, and V. Lepetit, "Keypoint transformer: Solving joint identification in challenging hands and object interactions for accurate 3d pose estimation," in *CVPR*, 2022.
- [56] O. Taheri, N. Ghorbani, M. J. Black, and D. Tzionas, "Grab: A dataset of whole-body human grasping of objects," in *European Conference on Computer Vision (ECCV)*, 2020.
- [57] O. Taheri, V. Choutas, M. J. Black, and D. Tzionas, "Goal: Generating 4d whole-body motion for hand-object grasping," *arXiv preprint arXiv:2112.11454*, 2021.
- [58] Z. Fan, O. Taheri, D. Tzionas, M. Kocabas, M. Kaufmann, M. J. Black, and O. Hilliges, "Articulated objects in free-form hand interaction," *arXiv preprint arXiv:2204.13662*, 2022.
- [59] A. X. Chang, T. Funkhouser, L. Guibas, P. Hanrahan, Q. Huang, Z. Li, S. Savarese, M. Savva, S. Song, H. Su, J. Xiao, L. Yi, and F. Yu, "ShapeNet: An Information-Rich 3D Model Repository," Stanford University — Princeton University — Toyota Technological Institute at Chicago, Tech. Rep. arXiv:1512.03012 [cs.GR], 2015.
- [60] M. Savva, A. X. Chang, and P. Hanrahan, "Semantically-Enriched 3D Models for Common-sense Knowledge," *CVPR 2015 Workshop on Functionality, Physics, Intentionality and Causality*, 2015.
- [61] K. M. Jatavallabhula, E. Smith, J.-F. Lafleche, C. F. Tsang, A. Rozantsev, W. Chen, T. Xiang, R. Lebariedian, and S. Fidler, "Kaolin: A pytorch library for accelerating 3d deep learning research," *arXiv preprint arXiv:1911.05063*, 2019.
- [62] J. J. Park, P. Florence, J. Straub, R. Newcombe, and S. Lovegrove, "Deepsdf: Learning continuous signed distance functions for shape representation," in *Conference on Computer Vision and Pattern Recognition (CVPR)*, 2019.
- [63] C. Ferrari and J. F. Canny, "Planning optimal grasps," in *ICRA*, vol. 3, no. 4, 1992, p. 6.
- [64] K. Sohn, H. Lee, and X. Yan, "Learning structured output representation using deep conditional generative models," *Advances in Neural Information Processing Systems (NeurIPS)*, vol. 28, 2015.
- [65] T. Feix, J. Romero, H.-B. Schmedmayer, A. M. Dollar, and D. Kragic, "The grasp taxonomy of human grasp types," *IEEE Transactions on Human-Machine Systems*, vol. 46, no. 1, pp. 66–77, 2015.